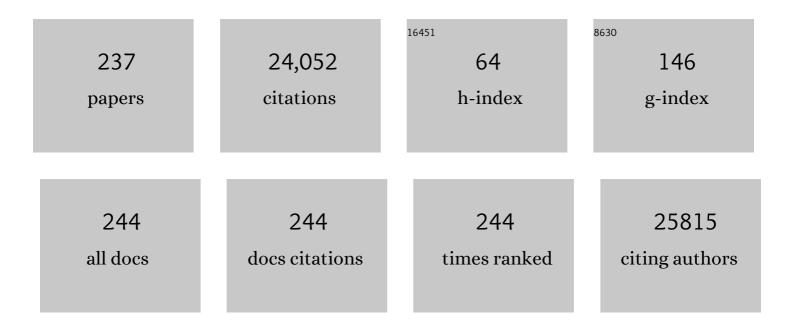
## Guido Gerig

List of Publications by Year in descending order

Source: https://exaly.com/author-pdf/6963720/publications.pdf Version: 2024-02-01



CHIDO GERIC

4

#	Article	IF	CITATIONS
1	A Prospective Evaluation of Infant Cerebellar-Cerebral Functional Connectivity in Relation to Behavioral Development in Autism Spectrum Disorder. Biological Psychiatry Global Open Science, 2023, 3, 149-161.	2.2	3
2	Infant Visual Brain Development and Inherited Genetic Liability in Autism. American Journal of Psychiatry, 2022, 179, 573-585.	7.2	14
3	Q-space Conditioned Translation Networks for Directional Synthesis of Diffusion Weighted Images from Multi-modal Structural MRI. Lecture Notes in Computer Science, 2021, , 530-540.	1.3	2
4	Equivariant Spherical Deconvolution: Learning Sparse Orientation Distribution Functions from Spherical Data. Lecture Notes in Computer Science, 2021, , 267-278.	1.3	5
5	Point-Supervised Segmentation Of Microscopy Images And Volumes Via Objectness Regularization. , 2021, , .		4
6	Segmentation-Renormalized Deep Feature Modulation for Unpaired Image Harmonization. IEEE Transactions on Medical Imaging, 2021, 40, 1519-1530.	8.9	21
7	Longitudinal Prediction of Infant MR Images With Multi-Contrast Perceptual Adversarial Learning. Frontiers in Neuroscience, 2021, 15, 653213.	2.8	4
8	Generative Adversarial Registration for Improved Conditional Deformable Templates. , 2021, , .		12
9	A Novel Method for High-Dimensional Anatomical Mapping of Extra-Axial Cerebrospinal Fluid: Application to the Infant Brain. Frontiers in Neuroscience, 2020, 14, 561556.	2.8	2
10	Sex differences associated with corpus callosum development in human infants: A longitudinal multimodal imaging study. NeuroImage, 2020, 215, 116821.	4.2	14
11	Multi-modal Perceptual Adversarial Learning for Longitudinal Prediction of Infant MR Images. Lecture Notes in Computer Science, 2020, , 284-294.	1.3	1
12	Trajectories from Distribution-Valued Functional Curves: A Unified Wasserstein Framework. Lecture Notes in Computer Science, 2020, , 343-353.	1.3	1
13	Self-supervised Denoising via Diffeomorphic Template Estimation: Application to Optical Coherence Tomography. Lecture Notes in Computer Science, 2020, , 72-82.	1.3	1
14	Hierarchical Geodesic Modeling on the Diffusion Orientation Distribution Function for Longitudinal DW-MRI Analysis. Lecture Notes in Computer Science, 2020, 12267, 311-321.	1.3	0
15	A Framework to Construct a Longitudinal DW-MRI Infant Atlas Based on Mixed Effects Modeling of dODF Coefficients. Mathematics and Visualization, 2020, 2020, 149-159.	0.6	2
16	User-Guided Segmentation of Multi-modality Medical Imaging Datasets with ITK-SNAP. Neuroinformatics, 2019, 17, 83-102.	2.8	97
17	Facilitating Manual Segmentation of 3D Datasets Using Contour And Intensity Guided Interpolation. , 2019, , .		6

Acceleration Controlled Diffeomorphisms For Nonparametric Image Regression. , 2019, 2019, 1488-1491.

#	Article	IF	CITATIONS
19	Tensor decomposition of hyperspectral images to study autofluorescence in age-related macular degeneration. Medical Image Analysis, 2019, 56, 96-109.	11.6	9
20	Rapid Radial T <sub>1</sub> and T <sub>2</sub> Mapping of the Hip Articular Cartilage With Magnetic Resonance Fingerprinting. Journal of Magnetic Resonance Imaging, 2019, 50, 810-815.	3.4	46
21	Restricted and Repetitive Behavior and Brain Functional Connectivity in Infants at Risk for Developing Autism Spectrum Disorder. Biological Psychiatry: Cognitive Neuroscience and Neuroimaging, 2019, 4, 50-61.	1.5	53
22	Multi-modal image fusion for multispectral super-resolution in microscopy. , 2019, 10949, .		7
23	Robust Non-negative Tensor Factorization, Diffeomorphic Motion Correction, and Functional Statistics to Understand Fixation in Fluorescence Microscopy. Lecture Notes in Computer Science, 2019, 11764, 658-666.	1.3	2
24	Hierarchical Multi-geodesic Model for Longitudinal Analysis of Temporal Trajectories of Anatomical Shape and Covariates. Lecture Notes in Computer Science, 2019, , 57-65.	1.3	5
25	Spatiotemporal Modeling for Image Time Series with Appearance Change: Application to Early Brain Development. Lecture Notes in Computer Science, 2019, , 174-185.	1.3	2
26	Model selection for spatiotemporal modeling of early childhood sub-cortical development. , 2019, 10949, .		1
27	Analysis of the kinematic motion of the wrist from 4D magnetic resonance imaging. , 2019, , .		2
28	Longitudinal structural connectivity in the developing brain with projective non-negative matrix factorization. , 2019, , .		1
29	Development of White Matter Circuitry in Infants With Fragile X Syndrome. JAMA Psychiatry, 2018, 75, 505.	11.0	35
30	Walking, Gross Motor Development, and Brain Functional Connectivity in Infants and Toddlers. Cerebral Cortex, 2018, 28, 750-763.	2.9	65
31	SlicerSALT: Shape AnaLysis Toolbox. Lecture Notes in Computer Science, 2018, 11167, 65-72.	1.3	20
32	Fully convolutional structured LSTM networks for joint 4D medical image segmentation. , 2018, , .		34
33	Estimating shape correspondence for populations of objects with complex topology. , 2018, 2018, 1010-1013.		3
34	4D continuous medial representation by geodesic shape regression. , 2018, 2018, 1014-1017.		3
35	4D Continuous Medial Representation Trajectory Estimation for Longitudinal Shape Analysis. Lecture Notes in Computer Science, 2018, , 125-136.	1.3	0
36	Analysis of Morphological Changes of Lamina Cribrosa Under Acute Intraocular Pressure Change. Lecture Notes in Computer Science, 2018, 11071, 364-371.	1.3	1

#	Article	IF	CITATIONS
37	A novel framework for the local extraction of extra-axial cerebrospinal fluid from MR brain images. , 2018, 10574, .		2
38	Splenium development and early spoken language in human infants. Developmental Science, 2017, 20, e12360.	2.4	36
39	Joint Attention and Brain Functional Connectivity in Infants and Toddlers. Cerebral Cortex, 2017, 27, 1709-1720.	2.9	103
40	Increased Extra-axial Cerebrospinal Fluid in High-Risk Infants Who Later Develop Autism. Biological Psychiatry, 2017, 82, 186-193.	1.3	173
41	Early brain development in infants at high risk for autism spectrum disorder. Nature, 2017, 542, 348-351.	27.8	808
42	Neural circuitry at age 6Âmonths associated with later repetitive behavior and sensory responsiveness in autism. Molecular Autism, 2017, 8, 8.	4.9	111
43	Functional neuroimaging of high-risk 6-month-old infants predicts a diagnosis of autism at 24 months of age. Science Translational Medicine, 2017, 9, .	12.4	264
44	Geodesic shape regression with multiple geometries and sparse parameters. Medical Image Analysis, 2017, 39, 1-17.	11.6	21
45	The Emergence of Network Inefficiencies in Infants With Autism Spectrum Disorder. Biological Psychiatry, 2017, 82, 176-185.	1.3	93
46	Spatiotemporal Analysis of Structural Changes of the Lamina Cribrosa. Lecture Notes in Computer Science, 2017, , 185-193.	1.3	1
47	Subject-specific longitudinal shape analysis by coupling spatiotemporal shape modeling with medial analysis. Proceedings of SPIE, 2017, 10133, .	0.8	1
48	Twin-singleton developmental study of brain white matter anatomy. Human Brain Mapping, 2017, 38, 1009-1024.	3.6	14
49	Resting-state fMRI in sleeping infants more closely resembles adult sleep than adult wakefulness. PLoS ONE, 2017, 12, e0188122.	2.5	51
50	Longitudinal Modeling of Multi-modal Image Contrast Reveals Patterns of Early BrainÂGrowth. Lecture Notes in Computer Science, 2017, , 75-83.	1.3	2
51	Performance of an efficient imageâ€registration algorithm in processing MR renography data. Journal of Magnetic Resonance Imaging, 2016, 43, 391-397.	3.4	6
52	Development of cortical shape in the human brain from 6 to 24months of age via a novel measure of shape complexity. NeuroImage, 2016, 135, 163-176.	4.2	33
53	Modeling 4D pathological changes by leveraging normative models. Computer Vision and Image Understanding, 2016, 151, 3-13.	4.7	2
54	Compressive sensing based Q-space resampling for handling fast bulk motion in hardi acquisitions. , 2016, 2016, 907-910.		4

#	Article	IF	CITATIONS
55	Image registration and segmentation in longitudinal MRI using temporal appearance modeling. , 2016, , .		7
56	ITK-SNAP: An interactive tool for semi-automatic segmentation of multi-modality biomedical images. , 2016, 2016, 3342-3345.		250
57	Longitudinal modeling of appearance and shape and its potential for clinical use. Medical Image Analysis, 2016, 33, 114-121.	11.6	20
58	Bayesian covariate selection in mixed-effects models for longitudinal shape analysis. , 2016, 2016, 656-659.		2
59	ND morphological contour interpolation. The Insight Journal, 2016, , .	0.2	11
60	RLEImage: run-length encoded memory compression scheme for an itk::Image. The Insight Journal, 2016, ,	0.2	1
61	Violence: heightened brain attentional network response is selectively muted in Down syndrome. Journal of Neurodevelopmental Disorders, 2015, 7, 15.	3.1	5
62	The DTI Challenge: Toward Standardized Evaluation of Diffusion Tensor Imaging Tractography for Neurosurgery. Journal of Neuroimaging, 2015, 25, 875-882.	2.0	147
63	Accurate age classification of 6 and 12 month-old infants based on resting-state functional connectivity magnetic resonance imaging data. Developmental Cognitive Neuroscience, 2015, 12, 123-133.	4.0	51
64	Shape index distribution based local surface complexity applied to the human cortex. Proceedings of SPIE, 2015, 9413, .	0.8	2
65	Altered corpus callosum morphology associated with autism over the first 2 years of life. Brain, 2015, 138, 2046-2058.	7.6	169
66	Automatic tissue segmentation of neonate brain MR Images with subject-specific atlases. Proceedings of SPIE, 2015, 9413, .	0.8	18
67	Prenatal Drug Exposure Affects Neonatal Brain Functional Connectivity. Journal of Neuroscience, 2015, 35, 5860-5869.	3.6	72
68	UNC-Utah NA-MIC framework for DTI fiber tract analysis. Frontiers in Neuroinformatics, 2014, 7, 51.	2.5	54
69	DTIPrep: quality control of diffusion-weighted images. Frontiers in Neuroinformatics, 2014, 8, 4.	2.5	221
70	Multi-atlas segmentation of subcortical brain structures via the AutoSeg software pipeline. Frontiers in Neuroinformatics, 2014, 8, 7.	2.5	98
71	A joint framework for 4D segmentation and estimation of smooth temporal appearance changes. , 2014, 2014, 1291-1294.		2
72	4D active cut: An interactive tool for pathological anatomy modeling. , 2014, 2014, 529-532.		18

5

#	Article	IF	CITATIONS
73	Characterizing growth patterns in longitudinal MRI using image contrast. , 2014, 9034, 90340D.		4
74	Parametric regression scheme for distributions: Analysis of DTI fiber tract diffusion changes in early brain development. , 2014, 2014, 559-562.		1
75	Subjectââ,¬â€œMotion Correction in HARDI Acquisitions: Choices and Consequences. Frontiers in Neurology, 2014, 5, 240.	2.4	12
76	Geodesic regression of image and shape data for improved modeling of 4D trajectories. , 2014, 2014, 385-388.		16
77	Morphometry of anatomical shape complexes with dense deformations and sparse parameters. NeuroImage, 2014, 101, 35-49.	4.2	195
78	Prenatal cocaine effects on brain structure in early infancy. NeuroImage, 2014, 101, 114-123.	4.2	49
79	Diffeomorphic Shape Trajectories for Improved Longitudinal Segmentation and Statistics. Lecture Notes in Computer Science, 2014, 17, 49-56.	1.3	10
80	Subject-Specific Prediction Using Nonlinear Population Modeling: Application to Early Brain Maturation from DTI. Lecture Notes in Computer Science, 2014, 17, 33-40.	1.3	6
81	Diffusion imaging quality control via entropy of principal direction distribution. NeuroImage, 2013, 82, 1-12.	4.2	18
82	Toward a Comprehensive Framework for the Spatiotemporal Statistical Analysis of Longitudinal Shape Data. International Journal of Computer Vision, 2013, 103, 22-59.	15.6	106
83	Abnormal brain synchrony in Down Syndrome. NeuroImage: Clinical, 2013, 2, 703-715.	2.7	111
84	Localized differences in caudate and hippocampal shape are associated with schizophrenia but not antipsychotic type. Psychiatry Research - Neuroimaging, 2013, 211, 1-10.	1.8	23
85	Regional characterization of longitudinal DT-MRI to study white matter maturation of the early developing brain. NeuroImage, 2013, 68, 236-247.	4.2	82
86	Adaptive prior probability and spatial temporal intensity change estimation for segmentation of the one-year-old human brain. Journal of Neuroscience Methods, 2013, 212, 43-55.	2.5	29
87	Associations between white matter microstructure and infants' working memory. Neurolmage, 2013, 64, 156-166.	4.2	90
88	UNC-Utah NA-MIC DTI framework: atlas based fiber tract analysis with application to a study of nicotine smoking addiction. Proceedings of SPIE, 2013, 8669, .	0.8	3
89	3D of brain shape and volume after cranial vault remodeling surgery for craniosynostosis correction in infants. , 2013, 8672, 86720V.		8
90	DTI quality control assessment via error estimation from Monte Carlo simulations. Proceedings of SPIE, 2013, 8669, 1667549.	0.8	5

#	Article	lF	CITATIONS
91	Modeling 4D Changes in Pathological Anatomy Using Domain Adaptation: Analysis of TBI Imaging Using a Tumor Database. Lecture Notes in Computer Science, 2013, 8159, 31-39.	1.3	8
92	White Matter Microstructure and Atypical Visual Orienting in 7-Month-Olds at Risk for Autism. American Journal of Psychiatry, 2013, 170, 899-908.	7.2	228
93	Analyzing imaging biomarkers for traumatic brain injury using 4d modeling of longitudinal MRI. , 2013, 2013, 1392-1395.		8
94	Spatiotemporal modeling of distribution-valued data applied to DTI tract evolution in infant neurodevelopment. , 2013, 2013, 684-687.		2
95	Multivariate modeling of longitudinal MRI in early brain development with confidence measures. , 2013, , 1400-1403.		10
96	Frontolimbic neural circuitry at 6Âmonths predicts individual differences in joint attention at 9Âmonths. Developmental Science, 2013, 16, 186-197.	2.4	77
97	Geodesic Shape Regression in the Framework of Currents. Lecture Notes in Computer Science, 2013, 23, 718-729.	1.3	19
98	Geodesic Image Regression with a Sparse Parameterization of Diffeomorphisms. Lecture Notes in Computer Science, 2013, 8085, 95-102.	1.3	4
99	Differences in White Matter Fiber Tract Development Present From 6 to 24 Months in Infants With Autism. American Journal of Psychiatry, 2012, 169, 589-600.	7.2	555
100	Brain Volume Findings in 6-Month-Old Infants at High Familial Risk for Autism. American Journal of Psychiatry, 2012, 169, 601-608.	7.2	83
101	Statistical growth modeling of longitudinal DT-MRI for regional characterization of early brain development. , 2012, , 1507-1510.		5
102	Segmentation of serial MRI of TBI patients using personalized atlas construction and topological change estimation. , 2012, , 1152-1155.		16
103	Longitudinal growth modeling of discrete-time functions with application to DTI tract evolution in early neurodevelopment. , 2012, 2012, 1945-1400.		1
104	Automatic corpus callosum segmentation using a deformable active Fourier contour model. , 2012, 8317, .		16
105	A patient-specific segmentation framework for longitudinal MR images of traumatic brain injury. , 2012, 8314, 831402.		11
106	Measures for validation of DTI tractography. , 2012, 8314, .		4
107	3D Tensor Normalization for Improved Accuracy in DTI Tensor Registration Methods. Lecture Notes in Computer Science, 2012, , 170-179.	1.3	0
108	Differences in subcortical structures in young adolescents at familial risk for schizophrenia: A preliminary study. Psychiatry Research - Neuroimaging, 2012, 204, 68-74.	1.8	19

#	Article	IF	CITATIONS
109	Prenatal isolated mild ventriculomegaly is associated with persistent ventricle enlargement at ages 1 and 2. Early Human Development, 2012, 88, 691-698.	1.8	38
110	Quantitative tract-based white matter development from birth to age 2 years. NeuroImage, 2012, 61, 542-557.	4.2	179
111	Neuroimaging of structural pathology and connectomics in traumatic brain injury: Toward personalized outcome prediction. NeuroImage: Clinical, 2012, 1, 1-17.	2.7	111
112	Patient-Tailored Connectomics Visualization for the Assessment of White Matter Atrophy in Traumatic Brain Injury. Frontiers in Neurology, 2012, 3, 10.	2.4	53
113	Analysis of Longitudinal Shape Variability via Subject Specific Growth Modeling. Lecture Notes in Computer Science, 2012, 15, 731-738.	1.3	15
114	Topology Preserving Atlas Construction from Shape Data without Correspondence Using Sparse Parameters. Lecture Notes in Computer Science, 2012, 15, 223-230.	1.3	24
115	Mixed-Effects Shape Models for Estimating Longitudinal Changes in Anatomy. Lecture Notes in Computer Science, 2012, 7570, 76-87.	1.3	15
116	DTI registration in atlas based fiber analysis of infantile Krabbe disease. NeuroImage, 2011, 55, 1577-1586.	4.2	110
117	FADTTS: Functional analysis of diffusion tensor tract statistics. NeuroImage, 2011, 56, 1412-1425.	4.2	66
118	Synergy of Image Analysis for Animal and Human Neuroimaging Supports Translational Research on Drug Abuse. Frontiers in Psychiatry, 2011, 2, 53.	2.6	5
119	CENTS: Cortical enhanced neonatal tissue segmentation. Human Brain Mapping, 2011, 32, 382-396.	3.6	40
120	Comparison of Acute and Chronic Traumatic Brain Injury Using Semi-Automatic Multimodal Segmentation of MR Volumes. Journal of Neurotrauma, 2011, 28, 2287-2306.	3.4	55
121	Twin-Singleton Differences in Neonatal Brain Structure. Twin Research and Human Genetics, 2011, 14, 268-276.	0.6	20
122	Early Brain Overgrowth in Autism Associated With an Increase in Cortical Surface Area Before Age 2 Years. Archives of General Psychiatry, 2011, 68, 467.	12.3	384
123	Efficient Probabilistic and Geometric Anatomical Mapping Using Particle Mesh Approximation on GPUs. International Journal of Biomedical Imaging, 2011, 2011, 1-16.	3.9	5
124	Optimal Data-Driven Sparse Parameterization of Diffeomorphisms for Population Analysis. Lecture Notes in Computer Science, 2011, 22, 123-134.	1.3	21
125	Estimation of Smooth Growth Trajectories with Controlled Acceleration from Time Series Shape Data. Lecture Notes in Computer Science, 2011, 14, 401-408.	1.3	30
126	Genetic and environmental contributions to neonatal brain structure: A twin study. Human Brain Mapping, 2010, 31, 1174-1182.	3.6	115

IF # ARTICLE CITATIONS Quality control of diffusion weighted images. Proceedings of SPIE, 2010, 7628, . Spatio-temporal analysis of early brain development., 2010, 2010, 777-781. 128 6 Brain volumes in psychotic youth with schizophrenia and mood disorders. Journal of Psychiatry and 129 2.4 Neuroscience, 2010, 35, 229-236. Towards analysis of growth trajectory through multimodal longitudinal MR imaging., 2010, 7623, . 130 3 Changes of MR and DTI appearance in early human brain development. Proceedings of SPIE, 2010, 7623, . 0.8 132 Evaluation of DTI property maps as basis of DTI atlas building., 2010, 7623, . 3 Prenatal and Neonatal Brain Structure and White Matter Maturation in Children at High Risk for 88 Schizophrenia. American Journal of Psychiatry, 2010, 167, 1083-1091. A new framework for analyzing white matter maturation in early brain development., 2010, , 97-100. 134 12 Multi-Object Analysis of Volume, Pose, and Shape Using Statistical Discrimination. IEEE Transactions 49 on Pattern Analysis and Machine Intelligence, 2010, 32, 652-661. Image Registration Driven by Combined Probabilistic and Geometric Descriptors. Lecture Notes in 136 1.3 6 Computer Science, 2010, 13, 602-609. Voxel-wise group analysis of DTI., 2009, , 807-810. Cortical enhanced tissue segmentation of neonatal brain MR images acquired by a dedicated phased 138 2 array coil., 2009,,. Longitudinal Study of Amygdala Volume and Joint Attention in 2- to 4-Year-Old Children With Autism. 12.3 199 Archives of General Psychiatry, 2009, 66, 509. Discordance of prenatal and neonatal brain development in twins. Early Human Development, 2009, 85, 140 1.8 7 171-175. Teasing apart the heterogeneity of autism: Same behavior, different brains in toddlers with fragile X 141 3.1 93 syndrome and autism. Journal of Neurodevelopmental Disorders, 2009, 1, 81-90. Probabilistic white matter fiber tracking using particle filtering and von Misesâ€"Fisher sampling. 142 11.6 60 Medical Image Analysis, 2009, 13, 5-18. Simulation of brain tumors in MR images for evaluation of segmentation efficacy. Medical Image 11.6 Analysis, 2009, 13, 297-311. Spatiotemporal Atlas Estimation for Developmental Delay Detection in Longitudinal Datasets. Lecture 144 1.3 81 Notes in Computer Science, 2009, 12, 297-304.

#	Article	IF	CITATIONS
145	Group analysis of DTI fiber tract statistics with application to neurodevelopment. Neurolmage, 2009, 45, S133-S142.	4.2	180
146	Cortical enhanced tissue segmentation of neonatal brain MR images acquired by a dedicated phased array coil. , 2009, 2009, 39-45.		1
147	Particle Based Shape Regression of Open Surfaces with Applications to Developmental Neuroimaging. Lecture Notes in Computer Science, 2009, 12, 167-174.	1.3	28
148	Constrained Data Decomposition and Regression for Analyzing Healthy Aging from Fiber Tract Diffusion Properties. Lecture Notes in Computer Science, 2009, 12, 321-328.	1.3	5
149	Offering to Share: How to Put Heads Together in Autism Neuroimaging. Journal of Autism and Developmental Disorders, 2008, 38, 2-13.	2.7	27
150	Prenatal Mild Ventriculomegaly Predicts Abnormal Development of the Neonatal Brain. Biological Psychiatry, 2008, 64, 1069-1076.	1.3	69
151	Multivariate nonlinear mixed model to analyze longitudinal image data: MRI study of early brain development. , 2008, , .		3
152	A Structural MRI Study of Human Brain Development from Birth to 2 Years. Journal of Neuroscience, 2008, 28, 12176-12182.	3.6	926
153	Minimum description length with local geometry. , 2008, , .		7
154	Multivariate longitudinal statistics for neonatal-pediatric brain tissue development. Proceedings of SPIE, 2008, , .	0.8	2
155	Group Statistics of DTI Fiber Bundles Using Spatial Functions of Tensor Measures. Lecture Notes in Computer Science, 2008, 11, 1068-1075.	1.3	10
156	Assessment of Reliability of Multi-site Neuroimaging Via Traveling Phantom Study. Lecture Notes in Computer Science, 2008, 11, 263-270.	1.3	28
157	Brain Lesion Segmentation through Physical Model Estimation. Lecture Notes in Computer Science, 2008, , 562-571.	1.3	6
158	CORRESPONDENCE EVALUATION IN LOCAL SHAPE ANALYSIS AND STRUCTURAL SUBDIVISION. , 2007, , .		12
159	Statistical Shape Analysis of Multi-Object Complexes. , 2007, , .		19
160	Statistical group differences in anatomical shape analysis using Hotelling T2 metric. , 2007, , .		6
161	Subcortical structure segmentation using probabilistic atlas priors. , 2007, , .		36
162	Discrimination analysis using multi-object statistics of shape and pose. , 2007, , .		3

#	Article	IF	CITATIONS
163	Diffusion Tensor Imaging. Journal of the American Academy of Child and Adolescent Psychiatry, 2007, 46, 213-223.	0.5	150
164	Regional Gray Matter Growth, Sexual Dimorphism, and Cerebral Asymmetry in the Neonatal Brain. Journal of Neuroscience, 2007, 27, 1255-1260.	3.6	389
165	Asymmetrical ventricular enlargement in Parkinson's disease. Movement Disorders, 2007, 22, 1657-1660.	3.9	11
166	Quantification of Measurement Error in DTI: Theoretical Predictions and Validation. , 2007, 10, 10-17.		8
167	Probabilistic Fiber Tracking Using Particle Filtering. , 2007, 10, 144-152.		10
168	Structural integrity of the uncinate fasciculus in geriatric depression: Relationship with age of onset. Neuropsychiatric Disease and Treatment, 2007, 3, 669-74.	2.2	71
169	User-guided 3D active contour segmentation of anatomical structures: Significantly improved efficiency and reliability. NeuroImage, 2006, 31, 1116-1128.	4.2	6,669
170	Cortical Gray and White Brain Tissue Volume in Adolescents and Adults with Autism. Biological Psychiatry, 2006, 59, 1-6.	1.3	155
171	Reduced Relationship to Cortical White Matter Volume Revealed by Tractography-Based Segmentation of the Corpus Callosum in Young Children With Developmental Delay. American Journal of Psychiatry, 2006, 163, 2157-2163.	7.2	22
172	Aggression and Quantitative MRI Measures of Caudate in Patients With Chronic Schizophrenia or Schizoaffective Disorder. Journal of Neuropsychiatry and Clinical Neurosciences, 2006, 18, 509-515.	1.8	38
173	Multi-modal image set registration and atlas formation. Medical Image Analysis, 2006, 10, 440-451.	11.6	91
174	Fiber tract-oriented statistics for quantitative diffusion tensor MRI analysis. Medical Image Analysis, 2006, 10, 786-798.	11.6	149
175	Improved Correspondence for DTI Population Studies Via Unbiased Atlas Building. Lecture Notes in Computer Science, 2006, 9, 260-267.	1.3	36
176	Framework for the Statistical Shape Analysis of Brain Structures using SPHARM-PDM. The Insight Journal, 2006, , 242-250.	0.2	154
177	KWMeshVisu: A Mesh Visualization Tool for Shape Analysis. The Insight Journal, 2006, , .	0.2	3
178	Framework for the Statistical Shape Analysis of Brain Structures using SPHARM-PDM. The Insight Journal, 2006, , .	0.2	107
179	Duration of illness and treatment effects on hippocampal volume in male patients with schizophrenia. British Journal of Psychiatry, 2005, 186, 26-31.	2.8	127
180	Automatic segmentation of MR images of the developing newborn brain. Medical Image Analysis, 2005, 9, 457-466.	11.6	306

#	Article	IF	CITATIONS
181	Assessment of mandibular growth and response to orthopedic treatment with 3-dimensional magnetic resonance images. American Journal of Orthodontics and Dentofacial Orthopedics, 2005, 128, 16-26.	1.7	51
182	Comparison of relative mandibular growth vectors with high-resolution 3-dimensional imaging. American Journal of Orthodontics and Dentofacial Orthopedics, 2005, 128, 27-34.	1.7	39
183	Quantitative MRI measures of orbitofrontal cortex in patients with chronic schizophrenia or schizoaffective disorder. Psychiatry Research - Neuroimaging, 2005, 140, 133-145.	1.8	79
184	Hypothesis Testing with Nonlinear Shape Models. Lecture Notes in Computer Science, 2005, 19, 15-26.	1.3	16
185	Morphometric analysis of lateral ventricles in schizophrenia and healthy controls regarding genetic and disease-specific factors. Proceedings of the National Academy of Sciences of the United States of America, 2005, 102, 4872-4877.	7.1	146
186	Magnetic Resonance Imaging and Head Circumference Study of Brain Size in Autism. Archives of General Psychiatry, 2005, 62, 1366.	12.3	577
187	Synthetic Ground Truth for Validation of Brain Tumor MRI Segmentation. Lecture Notes in Computer Science, 2005, 8, 26-33.	1.3	36
188	Vessel Tortuosity and Brain Tumor Malignancy. Academic Radiology, 2005, 12, 1232-1240.	2.5	239
189	Facial emotion perception and fusiform gyrus volume in first episode schizophrenia. Schizophrenia Research, 2005, 79, 341-343.	2.0	9
190	Fiber Tract-Oriented Statistics for Quantitative Diffusion Tensor MRI Analysis. Lecture Notes in Computer Science, 2005, 8, 131-139.	1.3	16
191	Effects of Healthy Aging Measured By Intracranial Compartment Volumes Using a Designed MR Brain Database. Lecture Notes in Computer Science, 2005, 8, 383-391.	1.3	29
192	A Quantitative DTI Fiber Tract Analysis Suite. The Insight Journal, 2005, , .	0.2	1
193	Analysis of brain white matter via fiber tract modeling. , 2004, 2004, 4421-4.		80
194	Abnormal Vessel Tortuosity as a Marker of Treatment Response of Malignant Gliomas: Preliminary Report. Technology in Cancer Research and Treatment, 2004, 3, 577-584.	1.9	39
195	3 Tesla magnetic resonance imaging of the brain in newborns. Psychiatry Research - Neuroimaging, 2004, 132, 81-85.	1.8	53
196	A brain tumor segmentation framework based on outlier detection*1. Medical Image Analysis, 2004, 8, 275-283.	11.6	498
197	Boundary and medial shape analysis of the hippocampus in schizophrenia. Medical Image Analysis, 2004, 8, 197-203.	11.6	224
198	Unbiased diffeomorphic atlas construction for computational anatomy. NeuroImage, 2004, 23, S151-S160.	4.2	766

#	Article	IF	CITATIONS
199	Correction scheme for multiple correlated statistical tests in local shape analysis. , 2004, , .		3
200	Automatic Segmentation of Neonatal Brain MRI. Lecture Notes in Computer Science, 2004, , 10-17.	1.3	22
201	Profile Scale-Spaces for Multiscale Image Match. Lecture Notes in Computer Science, 2004, , 176-183.	1.3	6
202	Determining Malignancy of Brain Tumors by Analysis of Vessel Shape. Lecture Notes in Computer Science, 2004, , 645-653.	1.3	7
203	Automatic and Robust Computation of 3D Medial Models Incorporating Object Variability. International Journal of Computer Vision, 2003, 55, 107-122.	15.6	63
204	Object models in multiscale intrinsic coordinates via m-reps. Image and Vision Computing, 2003, 21, 5-15.	4.5	9
205	Structural and radiometric asymmetry in brain images. Medical Image Analysis, 2003, 7, 155-170.	11.6	37
206	Automatic brain tumor segmentation by subject specific modification of atlas priors1. Academic Radiology, 2003, 10, 1341-1348.	2.5	246
207	Practical consideration for 3T imaging. Magnetic Resonance Imaging Clinics of North America, 2003, 11, 615-639.	1.1	44
208	MICCAI: medical image computing and computer-assisted intervention1. Academic Radiology, 2003, 10, 1339-1340.	2.5	2
209	Analysis Tool for Diffusion Tensor MRI. Lecture Notes in Computer Science, 2003, , 967-968.	1.3	23
210	Measuring tortuosity of the intracerebral vasculature from MRA images. IEEE Transactions on Medical Imaging, 2003, 22, 1163-1171.	8.9	339
211	Robust Estimation for Brain Tumor Segmentation. Lecture Notes in Computer Science, 2003, , 530-537.	1.3	29
212	Comparisons of Regional White Matter Diffusion in Healthy Neonates and Adults Performed with a 3.0-T Head-only MR Imaging Unit. Radiology, 2003, 229, 673-681.	7.3	79
213	Boundary and Medial Shape Analysis of the Hippocampus in Schizophrenia. Lecture Notes in Computer Science, 2003, , 464-471.	1.3	12
214	Quantitative Analysis of White Matter Fiber Properties along Geodesic Paths. Lecture Notes in Computer Science, 2003, , 16-23.	1.3	24
215	Age and Treatment Related Local Hippocampal Changes in Schizophrenia Explained by a Novel Shape Analysis Method. Lecture Notes in Computer Science, 2003, , 653-660.	1.3	4
216	Vascular Attributes and Malignant Brain Tumors. Lecture Notes in Computer Science, 2003, , 671-679.	1.3	12

#	Article	IF	CITATIONS
217	Scale-Space on Image Profiles about an Object Boundary. Lecture Notes in Computer Science, 2003, , 564-575.	1.3	5
218	Multisite validation of image analysis methods: assessing intra- and intersite variability. , 2002, 4684, 278.		33
219	Automatic Brain and Tumor Segmentation. Lecture Notes in Computer Science, 2002, , 372-379.	1.3	59
220	Amygdala–hippocampal shape differences in schizophrenia: the application of 3D shape models to volumetric MR data. Psychiatry Research - Neuroimaging, 2002, 115, 15-35.	1.8	121
221	Valmet: A New Validation Tool for Assessing and Improving 3D Object Segmentation. Lecture Notes in Computer Science, 2001, , 516-523.	1.3	180
222	Computer-assisted Visualization of Arteriovenous Malformations on the Home Personal Computer. Neurosurgery, 2001, 48, 576-583.	1.1	32
223	Infant cerebral ventricle volume: a comparison of 3-D ultrasound and magnetic resonance imaging. Ultrasound in Medicine and Biology, 2001, 27, 1143-1146.	1.5	58
224	Shape versus Size: Improved Understanding of the Morphology of Brain Structures. Lecture Notes in Computer Science, 2001, , 24-32.	1.3	90
225	Exploring the discrimination power of the time domain for segmentation and characterization of active lesions in serial MR data. Medical Image Analysis, 2000, 4, 31-42.	11.6	55
226	3D Graph Description of the Intracerebral Vasculature from Segmented MRA and Tests of Accuracy by Comparison with X-ray Angiograms. Lecture Notes in Computer Science, 1999, , 308-321.	1.3	36
227	Three-dimensional multi-scale line filter for segmentation and visualization of curvilinear structures in medical images. Medical Image Analysis, 1998, 2, 143-168.	11.6	999
228	Segmentation of 2-D and 3-D objects from MRI volume data using constrained elastic deformations of flexible Fourier contour and surface models. Medical Image Analysis, 1996, 1, 19-34.	11.6	212
229	Parametrization of Closed Surfaces for 3-D Shape Description. Computer Vision and Image Understanding, 1995, 61, 154-170.	4.7	545
230	Image analysis and computer vision in medicine. Computerized Medical Imaging and Graphics, 1994, 18, 85-96.	5.8	29
231	<title>Structural description and combined 3D display for superior analysis of cerebral vascularity&lt;br&gt;from MRA</title> . , 1994, , .		14
232	Temporal lobe sulco-gyral pattern anomalies in schizophrenia: an in vivo MR three-dimensional surface rendering study. Neuroscience Letters, 1994, 182, 7-12.	2.1	93
233	Unsupervised tissue type segmentation of 3D dual-echo MR head data. Image and Vision Computing, 1992, 10, 349-360.	4.5	83
234	Routine quantitative analysis of brain and cerebrospinal fluid spaces with MR imaging. Journal of Magnetic Resonance Imaging, 1992, 2, 619-629.	3.4	224

#	Article	IF	CITATIONS
235	Semiautomated ROI Analysis in Dynamic MR Studies. Part II. Journal of Computer Assisted Tomography, 1991, 15, 733-741.	0.9	28
236	Semiautomated ROI Analysis in Dynamic MR Studies. Part I. Journal of Computer Assisted Tomography, 1991, 15, 725-732.	0.9	30
237	<title>A Hardware And Software Optimized Program System For Interactive Image&lt;br&gt;Processing</title> . Proceedings of SPIE, 1984, , .	0.8	3